THE JOURNAL OF BIOLOGICAL CHEMISTRY VOL. 289, NO. 22, pp. 15413–15425, May 30, 2014

Atypical OmpR/PhoB Subfamily Response Regulator GlnR of Actinomycetes Functions as a Homodimer, Stabilized by the Unphosphorylated Conserved Asp-focused Charge Interactions*

Received for publication, December 23, 2013, and in revised form, March 18, 2014 Published, JBC Papers in Press, April 14, 2014, DOI 10.1074/jbc.M113.543504

Wei Lin (林炜)[‡], Ying Wang (王颖)[‡§], Xiaobiao Han (韩小彪)[‡], Zilong Zhang (张子龙)[‡], Chengyuan Wang (王程远)[¶], Jin Wang (王金)[‡], Huaiyu Yang (阳怀宇)[‖], Yinhua Lu (芦银华)[‡], Weihong Jiang (姜卫红)[‡], Guo-Ping Zhao (赵国屏)[‡§‡‡1], and Peng Zhang (张鹏)[‡¶2]**

*From the [‡]Chinese Academy of Sciences Key Laboratory of Synthetic Biology, [¶]State Key Laboratory of Plant Molecular Genetics, Institute of Plant Physiology and Ecology, Shanghai Institutes for Biological Sciences, Chinese Academy of Sciences, Shanghai 200032, China, the [§]State Key Laboratory of Genetic Engineering, Department of Microbiology and Microbial Engineering, School of Life Sciences, Fudan University, Shanghai 200433, China, the **Shanghai-MOST Key Laboratory of Disease and Health Genomics, Chinese National Human Genome Center at Shanghai, Shanghai 201203, China, the [‡‡]Department of Microbiology and Li Ka Shing Institute of Health Sciences, Chinese University of Hong Kong, Prince of Wales Hospital, Shatin, New Territories, Hong Kong SAR, China, and the [‖]Institute of Materia Medica, Chinese Academy of Sciences, Shanghai 201203, China*

Background: Orphan response transcription factor GlnR regulates nitrogen metabolism in important actinomycetes.
Results: GlnR has no typical "phosphorylation pocket," where the only conserved Asp is unphosphorylated but is essential for functional homodimerization.
Conclusion: Actinomycete GlnR is an atypical response regulator functioning as a homodimer.
Significance: Conserved Asp-focused charge interactions of actinomycete GlnR are probably the mechanism that stabilizes the homodimer for physiological function.

The OmpR/PhoB subfamily protein GlnR of actinomycetes is an orphan response regulator that globally coordinates the expression of genes related to nitrogen metabolism. Biochemical and genetic analyses reveal that the functional GlnR from *Amycolatopsis mediterranei* is unphosphorylated at the potential phosphorylation Asp^{50} residue in the N-terminal receiver domain. The crystal structure of this receiver domain demonstrates that it forms a homodimer through the α4-β5-α5 dimer interface highly similar to the phosphorylated typical response regulator, whereas the so-called "phosphorylation pocket" is not conserved, with its space being occupied by an Arg^{52} from the β3-α3 loop. Both *in vitro* and *in vivo* experiments confirm that GlnR forms a functional homodimer via its receiver domain and suggest that the charge interactions of Asp^{50} with the highly conserved Arg^{52} and Thr^{9} in the receiver domain may be crucial in maintaining the proper conformation for homodimerization, as also supported by molecular dynamics simulations of the wild type GlnR *versus* the deficient mutant GlnR(D50A). This model is backed by the distinct phenotypes of the total deficient GlnR(R52A/T9A) double mutant *versus* the single mutants of GlnR (*i.e.* D50N, D50E, R52A and T9A), which have only minor effects upon both dimerization and physiological function of GlnR *in vivo*, albeit their DNA binding ability is weakened compared with that of the wild type. By integrating the supportive data of GlnRs from the model *Streptomyces coelicolor* and the pathogenic *Mycobacterium tuberculosis*, we conclude that the actinomycete GlnR is atypical with respect to its unphosphorylated conserved Asp residue being involved in the critical Arg/Asp/Thr charge interactions, which is essential for maintaining the biologically active homodimer conformation.

A two-component system, typically consisting of a membrane-associated sensor histidine kinase and a cognate intracellular response regulator (RR),[3] is the predominant signal transduction system employed by bacteria, and also found in archaea and eukarya (1). Most typical RRs remain as monomers or "weak" dimers (2, 3) with their receiver domains unphosphorylated. Once the environmental stimulus triggers histidine kinase autophosphorylation, the phosphoryl group is transferred to a conserved Asp residue in the receiver domain of the cognate RR. The phosphorylated RR then undergoes a substantial conformational change for "tight" homodimerization that enables its binding to the target DNA sequences (*cis*-elements) and in turn affects the transcription (4–6). Based on the homology of their DNA-binding domains, most RRs can be categorized into four major subfamilies (*i.e.* OmpR/PhoB, NarL/FixJ,

* This work is supported by National Basic Research Program of China Grant 2012CB721102; National Nature Science Foundation Grants 31322016, 31121001, and 30830002; and Shanghai Institutes for Biological Sciences, Chinese Academy of Sciences, Grants 2012OHTP, 2009CSP001, and KSCX2-EW-J-12.

The atomic coordinates and structure factors (codes 4O1H and 4O1I) have been deposited in the Protein Data Bank (http://wwpdb.org/).

[1] To whom correspondence may be addressed. E-mail: gpzhao@sibs.ac.cn.
[2] To whom correspondence may be addressed. E-mail: pengzhang01@sibs.ac.cn.

[3] The abbreviations used are: RR, response regulator; GlnRRec, GlnR regulatory domain; DSS, disuccinimidyl suberate; Bistris propane, 1,3-bis[tris(hydroxymethyl)methylamino]propane; MD, molecular dynamics; FAM, 6-carboxyfluorescein.

NtrC, and LytR), leaving the remaining RRs containing miscellaneous effector domains, such as RNA binding or enzymatic functions (2, 7).

In most bacteria, a two-component system is employed to sense and respond to the nitrogen status in the environment, and the NtrB/NtrC-mediated nitrogen assimilation regulation in enteric bacteria is one of the best studied (8, 9). However, in many actinomycetes, including the rifamycin-producing industrial actinomycete *Amycolatopsis mediterranei*, the model organism *Streptomyces coelicolor*, and the pathogenic *Mycobacterium tuberculosis*, nitrogen assimilation is globally regulated by an OmpR/PhoB subfamily protein, GlnR (10–13), which is considered an orphan RR because its cognate sensor histidine kinase has not been identified (10, 11, 14–16). Despite its great importance in global regulation of nitrogen metabolism, the understanding of the regulation of GlnR activity as well as its impact upon the GlnR-mediated global transcription regulation is limited, although much attention has been paid to the identification of the GlnR target genes and their corresponding *cis*-elements so far (10, 13, 17–19) .

The GlnR from *S. coelicolor* (ScoGlnR) was once predicted to be a typical RR subject to Asp phosphorylation as typical OmpR/PhoB subfamily members due to the presence of the conserved residues Asp^{50} and Thr^{83} of the active site quintet (14, 20, 21), essential in defining the so-called acidic "phosphorylation pocket" of the typical RRs (22). Recently, the atypical receiver domains of several orphan RRs (7, 22, 23) were shown to be generally similar to the typical receiver domains in their amino acid sequences and three-dimensional structures but lacked one or more residues of the highly conserved active site quintet (22, 24). Because the GlnR from actinomycetes other than streptomycetes (see Fig. 2) only has its putative phosphorylation site Asp residue found to be conserved in the active quintet (21, 25), we hypothesized that GlnR is an atypical RR, with its activity being independent of Asp phosphorylation. However, this hypothesis was mechanistically challenged by a mutational analysis, in which substitution of the potential phosphorylation site Asp residue with Ala abolished the GlnR function in *Mycobacterium smegmatis* (14).

In this study, the structure-function relationship of GlnR from *A. mediterranei* (AmeGlnR) is comprehensively analyzed. By integration of the knowledge learned from those of *M. tuberculosis* and *S. coelicolor*, the conserved Asp site of actinomycete GlnR is proved to be unphosphorylated but critical for homodimerization via its charge interactions with the surrounding residues, which, in turn, are essential for its physiological function *in vivo* and DNA binding ability *in vitro*.

EXPERIMENTAL PROCEDURES

Bacterial Strains, Plasmids, and Growth Conditions—*Escherichia coli* strains were grown at 37 °C in lysogeny broth (LB) medium (26). *A. mediterranei* were grown at 30 °C in the nutrient-rich Bennett's medium (27). To examine the growth phenotypes of *A. mediterranei* U32 and its *glnR* mutants, strains were incubated at 30 °C in minimal medium (27) supplemented with 80 mM potassium nitrate or 60 mM ammonium sulfate as the sole nitrogen source, and the growth was observed after 7 days' cultivation. *S. coelicolor* M145 and its derivatives were generally cultured at 30 °C in the MS medium for spore suspension preparations (28), whereas phenotype analysis was conducted in nitrogen-limited N-Evans medium with 5 mM nitrate or 100 mM ammonium sulfate as the sole nitrogen source after 4 days' cultivation. If necessary, the media were supplemented with antibiotics (100 μg ml^{-1} for ampicillin, 50 μg ml^{-1} for kanamycin, 50 μg ml^{-1} for apramycin, and 50 μg ml^{-1} for thiostrepton).

Expression and Purification of GlnR Regulatory Domain (GlnRRec) Protein—DNA fragments encoding the receiver domains of GlnR proteins were PCR-amplified using the genomic DNA of *A. mediterranei* U32 (*AmeglnRRec*) and *M. tuberculosis* H37Rv (*MtbglnRRec*). The PCR products were digested and inserted into the pET28b expression vector, resulting in N-terminal His_6-tagged pET-28bAmeglnRRec and pET-28bMtbglnRRec. The plasmid was transformed into *E. coli* BL21 (DE3) strain (Novagen), and the cells were cultured at 37 °C in LB medium containing 50 μg ml^{-1} kanamycin. Protein expression was induced by adding isopropyl β-D-thiogalactoside into the medium to a final concentration of 1 mM, when the A_{600} is 0.8. Then the cells were harvested by centrifugation at 5,000 $\times$ *g* for 10 min at 4 °C, resuspended in a lysis buffer (50 mM Tris-HCl, pH 8.0, 100 mM NaCl, and 1 mM PMSF), and disrupted using a French press. The recombinant protein was purified with affinity chromatography using a Ni^{2+}-nitrilotriacetate Superflow column (Qiagen) pre-equilibrated with buffer A (50 mM Tris-HCl, pH 8.0, and 100 mM NaCl) and then washed with buffer B (buffer A supplemented with 50 mM imidazole) to remove nonspecific binding proteins. The target protein was eluted with buffer C (buffer A supplemented with 250 mM imidazole), and the eluted fractions were further purified using a gel filtration column (GE Healthcare). After the two-step purification, the target protein was of sufficient purity (above 95%) and was then concentrated to ~10 mg ml^{-1} in buffer A by ultrafiltration for further structural and biochemical studies.

Selenomethionine-substituted AmeGlnRRec protein was prepared following a method described previously (29). Purification of the selenomethionine AmeGlnRRec protein was performed using the same methods as for the native protein. Gel filtration analysis of the purified protein was performed to measure the oligomeric state of AmeGlnRRec in solution. High and low molecular weight (mass) calibration kits (GE Healthcare) were used to calibrate the molecular mass of wild type and mutants of AmeGlnRRec. All of the above analysis was carried out on an FPLC system (GE Healthcare). Protein samples of 100 μl each were loaded into a 0.5-ml sample loop and injected into a Superdex 200 column. The apparent molecular mass of the protein sample was calculated according to the protocol provided in the kit.

Phos-tag Acrylamide Gel Analysis of GlnR Phosphorylation—For sample preparation for *in vivo* detection of phosphorylation, a standard protocol was used with minor modifications (30). *A. mediterranei* U32 or *S. coelicolor* M145 and related mutants were grown in Bennett's or MS medium (10) at 30 °C for 2 days and were then harvested by swabbing from the plate. Aliquots of the cells were washed and resuspended in minimal medium or N-Evans medium supplemented with 80 mM potas-

sium nitrate or 60 mM ammonium sulfate as the sole nitrogen source for GlnR or with 4 or 0 mM potassium hydrogen phosphate as the sole phosphate source for AmePhoP. After 12 h of growth, cells were pelleted by centrifugation, immediately following harvest; cells were lysed with 3.3 ml of 1 M formic acid (0.55 M final concentration formic acid) per equivalent of pellet of 50 ml of 0.2 A_{600} of cells. A French press was used to lyse the frozen cell pellet. Each lysate was solubilized by the addition of 200 μl of 5 M NaOH (0.17 M final concentration) to neutralize the solution and 1.5 ml of 5× SDS loading solution. Resulting cell lysates (20 μl) were immediately loaded onto a Phos-tag gel for electrophoresis as described below; the whole lysis process should be kept at a low temperature to prevent the hydrolysis of phospho-Asp residues.

For *in vitro* phosphorylation experiments, solutions of 10 μM protein in phosphorylation buffer (50 mM Tris-HCl, pH 8.0, 100 mM NaCl, 2 mM β-mercaptoethanol, 20 mM $MgCl_2$) with or without incubation with 20 mM ammonium hydrogen phosphoramidate (synthesized as described previously (31)) for 30 min at 37 °C were prepared. The phosphorylation reactions were stopped by the addition of 5× SDS-loading buffer. Phos-tag acrylamide gels were prepared as described previously with minor modifications (30, 32, 33). Phos-tag acrylamide running gels contained 12% (w/v) 29:1 acrylamide/*N*,*N*-methylene-bisacrylamide, 375 mM Tris, pH 8.8, 0.1% (w/v) SDS. Gels were copolymerized with 25 μM Phos-tag acrylamide and 50 μM $MnCl_2$ for analysis of purified GlnR and other positive control proteins. The stacking gels contained 5% (w/v) 29:1 acrylamide/*N*,*N*-methylene-bisacrylamide, 125 mM Tris, pH 6.8, 0.1% (w/v) SDS. All Phos-tag acrylamide-containing gels were run at 4 °C under constant voltage (120 V). Gels were fixed for 10 min in standard transfer buffer (20% (v/v) methanol, 50 mM Tris-HCl, 40 mM glycine, with 1 mM EDTA added to remove Mn^{2+}) and then incubated for an additional 20 min in transfer buffer without EDTA to remove the chelated metal. Transfer to nitrocellulose membranes was performed using a Bio-Rad transfer apparatus under a constant 300 mA for 1 h. Western blotting assay was performed using standard protocols.

Crystallization, Data Collection, and Structure Determination—The AmeGlnRRec and MtbGlnRRec proteins were used in crystallization experiments at 4 °C using the sitting drop vapor diffusion method. Crystals were grown in the drop containing equal volumes (1 μl) of the protein solution (~10 mg/ml AmeGlnRRec/MtbGlnRRec) and the reservoir solution (0.1 M Tris-HCl, pH 8.0, and 20% MPD (1.8 M sodium acetate trihydrate, pH 7.0, 0.1 M Bistris propane)), respectively. For diffraction data collection, the AmeGlnRRec and MtbGlnRRec crystals were first cryoprotected using paratone oil (Hampton Research) and then flash-cooled in liquid nitrogen. Selenium single-wavelength anomalous dispersion and native data of AmeGlnRRec were collected to a resolution of 3.0 and 2.8 Å, respectively, from flash-cooled crystals at 100 K at the Shanghai Synchrotron Radiation Facility, beamline BL17U. The native data of MtbGlnRRec were collected to 2.8 Å. The diffraction data were processed, integrated, and scaled together using the HKL2000 suite.

Structure of the AmeGlnRRec was solved using the Autosol implemented in Phenix (34). Over 60% of main chain residues were built, and the overall figure of merit was increased from 0.35 to 0.69 at 3.0 Å. The full structure model was built manually using the program Coot (35). Structure refinement was carried out using Phenix and refmac. Because the resolution and statistics of the single wavelength anomalous dispersion data set of AmeGlnRRec were better than the native data, the single wavelength anomalous dispersion data set was used in the final refinement of the structure of AmeGlnRRec. The structure of MtbGlnRRec was solved by molecular replacement using the structure of AmeGlnRRec as a starting model. The final model was refined to 2.8 Å. All of the statistics of data collection and structure refinement are summarized in Table 1.

Molecular Dynamics Simulations—The starting structure of AmeGlnR monomer was extracted from the crystal structures of AmeGlnR dimer. The D50A, D50E, and D50N mutants were built from the wild type by mutating the aspartic acid into glutamate or asparagine, respectively. After that, each system was solvated by TIP3P waters with 0.15 M NaCl. Finally, each simulation system includes about 17,000 atoms (55 × 55 × 55 Å).

MD simulations were carried out with the GROMACS version 4.6.1 package with the NPT ensemble and periodic boundary condition (36). The AMBER99SB-ILDN force field was applied for the simulations (37). Energy minimizations were first performed to relieve unfavorable contacts, followed with 2 ns in total to equilibrate the side chains of protein and solvent. The particle mesh Ewald method was used for long range electrostatic interactions with a short range cut-off of 1.2 nm. All simulations were run at 300 K using the v-rescale method with a coupling time of 0.1 ps (38). The pressure was kept at 1 bar using the Berendsen barostat $\tau p = 1.0$ ps and a compressibility of 4.5×10^{-5} bar^{-1}. SETTLE constraints and LINCS constraints were applied on the hydrogen-involved covalent bonds in water molecules and in other molecules, respectively, and the time step was set to 2 fs. Each system was put into a 150-ns production run.

Electrophoretic Mobility Shift Assay (EMSA)—For expression of recombinant mutated AmeGlnR (*i.e.* D50A, D50N, T9A, R52A, T9A/R52A, R111A, and R111E mutants), the wild type *AmeglnR* gene on the expression plasmid pET28b was mutated using site-directed mutagenesis methods (18). The *glnA* promoter region of *A. mediterranei* U32 was generated by PCR and was then inserted into the HincII site of pUC18. The obtained plasmid was used as the template for preparation of the FAM-labeled probes using the universal primer pair of FAM-labeled M13F (−47) and M13R (−48). FAM-labeled probe (30 ng) was incubated with varying amounts of AmeGlnR or its mutants at 25 °C for 20 min in a buffer of 25 mM Tris-HCl (pH 8.0), 50 mM KCl, 2.5 mM $MgCl_2$, 5% glycerol, 1 mM dithiothreitol (DTT), and 100 $\mu g\ ml^{-1}$ sonicated salmon sperm DNA (Sangon) (total volume 20 μl). Because GlnR has been proved a specific regulator for binding of the *glnA* promoter region in *A. mediterranei* U32 (39) and the EMSA employed in this study is to measure the DNA binding affinities of GlnR as well as its mutants, the cold probe competition assay was unnecessary and was therefore omitted. The resulting DNA-protein complexes were subjected to electrophoresis on agarose gels with a running buffer containing 40 mM Tris-HCl (pH 7.8), 20 mM boric acid, and 1 mM EDTA at 150 V and 4 °C for 1 h. After electrophoresis,

gels were directly scanned for fluorescent DNA using an ImageQuant™ LAS 4000 system (GE Healthcare).

Complementation Assay—The *A. mediterranei glnR* gene together with its native promoter region was amplified from *A. mediterranei* genome DNA and ligated with pRT803, which was excised by EcoRV, yielding plasmid pRT803AmeglnR, which was then used as the template for site-directed mutagenesis of *AmeglnR*. After verification by DNA sequencing, the complementation plasmids were transformed into *A. mediterranei* U32Δ*glnR* using a Bio-Rad Gene Pulser according to the methods described previously (40). Transformants were selected in Bennett's agar plates containing hygromycin. The *S. coelicolor glnR* gene together with its native promoter region was excised from pSETScoglnR with BamHI (18) and was subsequently cloned into the same site of pBluescript II SK (Stratagene), yielding plasmid pSKScoglnR, which was then used as the template for site-directed mutagenesis of *scoglnR*. The generated plasmids with various mutations of *scoglnR* were digested with BamHI and inserted into the same site of pSET1521 (41) to obtain the relevant plasmids for *scoglnR* complementation. After being verified by DNA sequencing, the complementation plasmids were conjugated into *S. coelicolor* M145Δ*glnR* (18). Exconjugants were selected by growth on MS agar flooded with nalidixic acid and thiostrepton.

In Vivo Chemical Cross-linking Experiment—A. mediterranei strains containing the mutated residues in *glnR* were made by complementing the *A. mediterranei* U32Δ*glnR* strain with mutated *A. mediterranei glnR* fused with a FLAG tag at the C terminus using the method described above. *A. mediterranei* was first cultured in liquid Bennett's medium at 30 °C for 48 h before being inoculated into fresh liquid minimal medium supplemented with either 80 mM KNO_3 or 60 mM $(NH_4)_2SO_4$ for another 24-h culture. Cells were then collected, and the cell pellets were resuspended in PBS and exposed to 5 mM DSS (Pierce). After a 20-min incubation at 25 °C, the reaction was quenched with the addition of 50 mM Tris-HCl (pH 8.0) (final concentration) for 15 min. The samples were subjected to SDS-PAGE and immunoblot assays were performed using the anti-FLAG antibody.

Reverse Transcription PCR (RT-PCR)—For RNA extraction, wild type *A. mediterranei* U32 and *glnR* mutants were grown in liquid Bennett's medium for 48 h before being inoculated into fresh liquid Bennett's medium supplemented with 80 mM KNO_3 or 60 mM $(NH_4)_2SO_4$ for further culture for 36 h. Total RNA was extracted using TRIzol reagent (Invitrogen). RNA was treated with RNase-free DNase I (Promega) to prevent contamination of trace genomic DNA. Reverse transcription was performed with a random hexamer primer using 3 μg of RNA in a total volume of 30 μl employing Super-Script III reverse transcriptase (Invitrogen). PCR was performed employing 20-ng reaction mixtures as the template to check the transcription of *nasA* and *glnR* genes and using the *rpoB* gene as the internal control. A negative control was made by following the same procedures except that the addition of reverse transcriptase was omitted. Two independent samples were used for analyses.

RESULTS

GlnR of Either A. mediterranei or S. coelicolor Is Unphosphorylated at the Potential Asp Phosphorylation Site—Because the Phos-tag methods (30, 32, 33) are able to characterize the phosphorylation state of the Asp residues in typical RRs, such as that shown for PhoB from *E. coli* (EcoPhoB) cell lysates (42), similar *in vitro* phosphorylation assays employing the high energy phospho-donor, ammonium hydrogen phosphoramidate, against the purified recombinant proteins of AmeGlnR and ScoGlnR proteins were conducted individually. Both of the annotated typical RRs (*i.e.* PhoP of *A. mediterranei* (AmePhoP) (13) and SCO5403 of *S. coelicolor* (21)), bearing the highly conserved acidic quintet in their amino acid sequences, as well as the purified well characterized EcoPhoB could be successfully phosphorylated *in vitro* by ammonium hydrogen phosphoramidate, probably at their corresponding Asp residues, whereas neither AmeGlnR nor ScoGlnR could (Fig. 1*A*). Therefore, it is unlikely that the conserved Asp residues of either of the two GlnRs can be phosphorylated by the high energy phosphodonor *in vitro*.

In order to test whether GlnR is phosphorylated or not *in vivo*, the phosphorylation status of AmeGlnR or ScoGlnR *in vivo* was tested via Western blot analysis against the cell lysates of *A. mediterranei* or *S. coelicolor* electrophoresed on Phos-tag gel, employing AmePhoP as a positive control and AmePhoP-(D52A) as a negative control. In accord with the fact that the Asp^{52} of PhoP is phosphorylated under the phosphate limitation conditions (43), AmePhoP exhibited a single band on the gel when cells are grown in phosphate (K_2HPO4)-rich medium, whereas double bands of AmePhoP were observed for cells grown in phosphate-limiting media. Obviously, the upper band corresponding to the phosphorylated AmePhoP disappeared in the D52A mutation, indicating that Asp^{52} was the phosphorylation site (Fig. 1*B*). In contrast, although GlnR is functional under nitrogen-limited conditions (39), no phosphorylation band of AmeGlnR or ScoGlnR could be observed in lysates of cells grown in either nitrogen-rich ($(NH_4)_2SO_4$) or nitrogen-limited (KNO_3) media. All of these results are in good agreement with the results of the *in vitro* experiments mentioned above (Fig. 1*A*), and therefore, we conclude that both AmeGlnR and ScoGlnR are unphosphorylated at their conserved Asp residues.

Crystal Structures of the GlnR Receiver Domains from A. mediterranei and M. tuberculosis Are Distinct from That of the Typical RRs Regarding the Potential "Phosphorylation Pocket" and Its Surrounding Amino Acid Residues—We determined the crystal structures of the receiver domains of GlnR from *A. mediterranei* U32 (AmeGlnRRec) and *M. tuberculosis* (MtbGlnRRec). The final structure models of both proteins were refined to 2.8 Å, with their statistics summarized in Table 1. Considering that AmeGlnRRec and MtbGlnRRec not only share 58% sequence identity (Fig. 2*A*) but also form similar homodimer structures (root mean square deviation = 1.0 Å), AmeGlnRRec alone is selected for further structural and functional analyses (Fig. 2*B*). The structures of AmeGlnRRec and MtbGlnRRec have been deposited to the Protein Data Bank with the codes 4O1H and 4O1I, respectively.

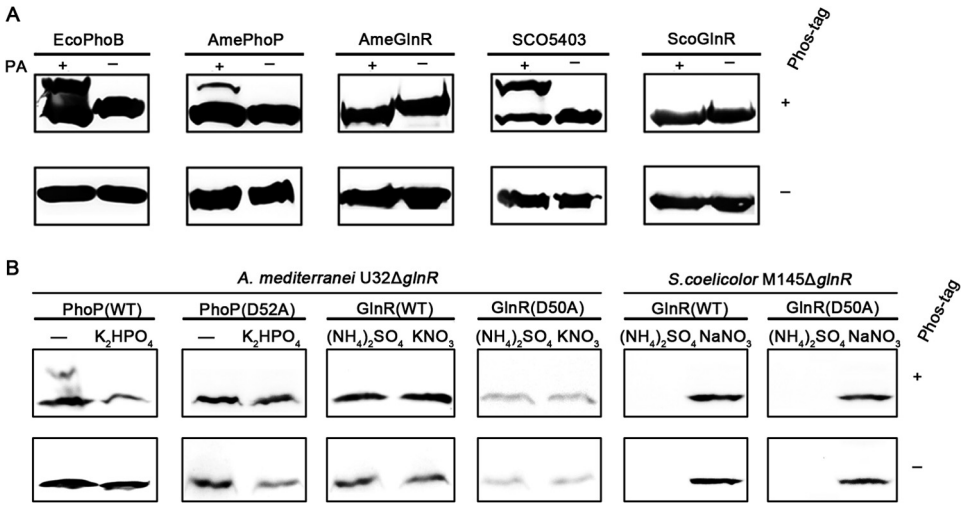

FIGURE 1. **Biochemical analyses detecting the phosphorylation status of the conserved residue Asp of GlnR.** *A*, Western blot monitoring the phosphorylation status of the His tag-fused *E. coli* PhoB (EcoPhoB), *S. coelicolor* GlnR/5403 (ScoGlnR/SCO5403), *A. mediterranei* U32 GlnR (AmeGlnR), and the *A. mediterranei* U32 PhoP (AmePhoP), purified by nickel affinity chromatography from the corresponding *E. coli* heterologous expression systems (see "Experimental Procedures") treated with (+) or without (−) 20 mM ammonium hydrogen phosphoramidate (*PA*). *B*, Western blot monitoring the *in vivo* phosphorylation status of the FLAG tag-fused PhoP (WT, D52A) under phosphate-replete (K_2HPO_4) or -limited (−) conditions and the phosphorylation status of FLAG tag-fused GlnR (WT, D50A) under nitrogen-rich ($(NH_4)_2SO_4$) or -limited (KNO_3) conditions in the *A. mediterranei* U32Δ*glnR* and *S. coelicolor* M145Δ*glnR* strains. Cell lysates were treated as described under "Experimental Procedures."

TABLE 1
Statistics of diffraction data collection and structure refinement

	MtbGlnRRec	AmeGlnRRec	AmeGlnRRec-Se
Diffraction data			
Wavelength (Å)	0.9793	0.9793	0.9793
Space group	I41	$P6_522$	$P6_522$
Cell parameters			
a (Å)	144.2	93.1	93.1
b (Å)	144.2	93.1	93.1
c (Å)	92.2	308.4	310.4
α (degrees)	90.0	90.0	90
β (degrees)	90.0	90.0	90
γ (degrees)	90.0	120.0	120
Resolution (Å)	50.0–2.80 (2.90–2.80)[a]	50.0–2.80 (2.90–2.80)	50.0–3.00 (3.11–3.00)
Observed reflections	71,225	196,781	698891
Unique reflections ($I/\sigma(I) > 0$)	23,093	20,511	16,902
Average redundancy	3.1 (3.1)	9.6 (9.9)	41.3 (42.8)
Average I/σ (I)	13.7 (4.4)	19.1 (4.4)	54.8 (10.9)
Completeness (%)	99.0 (99.7)	99.8 (100.0)	100.0 (100.0)
R_{merge} (%)[b]	9.8 (31.9)	11.7 (62.1)	16.0 (63.0)
Refinement and structure model			
Reflections ($F_o \geq 0\sigma(F_o)$)			
Working set	21,918	19,390	
Test set	1,158	1,039	
R_{work}/R_{free} (%)[c]	18.0/22.5	22.1/26.9	
No. of atoms	4,283	3,391	
Protein	4,111	3,364	
Water	172	27	
Average *B* factor (Å^2)			
All atoms	38.8	54.5	
Protein	38.8	54.6	
Water	38.5	50.3	
Root mean square deviations			
Bond lengths (Å)	0.007	0.011	
Bond angles (degrees)	1.4	1.9	
Ramachandran plot (%)			
Most favored	95.3	97.6	
Allowed	4.7	2.4	

[a] Numbers in parentheses represent the highest resolution shell.
[b] $R_{merge} = \sum_{hkl}\sum_i I_i(hkl) - \langle I(hkl)\rangle|/\sum_{hkl}\sum_i I_i(hkl)$.
[c] $R = \sum_{hkl}||F_o| - |F_c||/\sum_{hkl}|F_o|$.

The structure of AmeGlnRRec consists of five alternating β-strands and α-helices folding into a five-stranded parallel β-sheet in the middle surrounded by two α-helices on one side and three on the other (Fig. 2*B*), which is similar to most of the known structures of the typical RR receiver domains (22) except that the helices α1, α2, and α4 of AmeGlnRRec are partially unwound (Fig. 2*C*). We notice that the so-called "phosphorylation pocket" defined in the typical RRs as well as its microenvironment are significantly altered in the structure of AmeGlnRRec (Fig. 2, *A* and *C*). All of the five residues essential for the phosphorylation of PhoB except Asp^{50} are neither conserved nor in proper position, which is also demonstrated by the structure-based sequence alignment among GlnR proteins from representative actinomycetes and the well characterized typical and atypical RRs from Gram-negative bacteria (Fig. 2*A*). The Glu^9 and Asp^{10} residues known to bind with Mg^{2+} to promote phosphorylation and dephosphorylation in PhoB of *E. coli* are replaced by residues Thr^9 and Ala^{10} in AmeGlnRRec, respectively. These changes are likely to exclude the binding of a divalent metal cation and hence reduce the possibility of phosphorylation at AmeGlnRRec residue Asp^{50}. In addition, the Thr and Lys residues believed to communicate between the phosphorylation site and dimer interface in typical RRs are changed to Val^{81} and Leu^{100}, respectively, and the critical conformation switch residue Tyr is also substituted with an Ile^{98} in AmeGlnRRec. These data suggest that the AmeGlnR is significantly diverged from the canonical RRs with respect to the potential "phosphorylation pocket" and its surrounding amino acid residues.

When the monomer structure of AmeGlnRRec is superimposed with that of the phosphorylated PhoB (root mean square deviation = 2.1 Å), we find that the β1-α1 and β3-α3 loops move toward the putative phosphorylation pocket, thus shrinking the size of the "pocket." It is particularly significant that the Arg^{52} residue, conserved among all GlnR proteins but completely different in Gram-negative OmpR/PhoB subfamily proteins (Fig. 2*A*), protrudes from the β3-α3 loop into and occupied the "pocket" with its guanidinium side chain positioned at the close vicinity of the carboxyl side chain of the only conserved Asp^{50}. Based on the measured distance of the interactions, an ionic bridge may form between the side chains of these

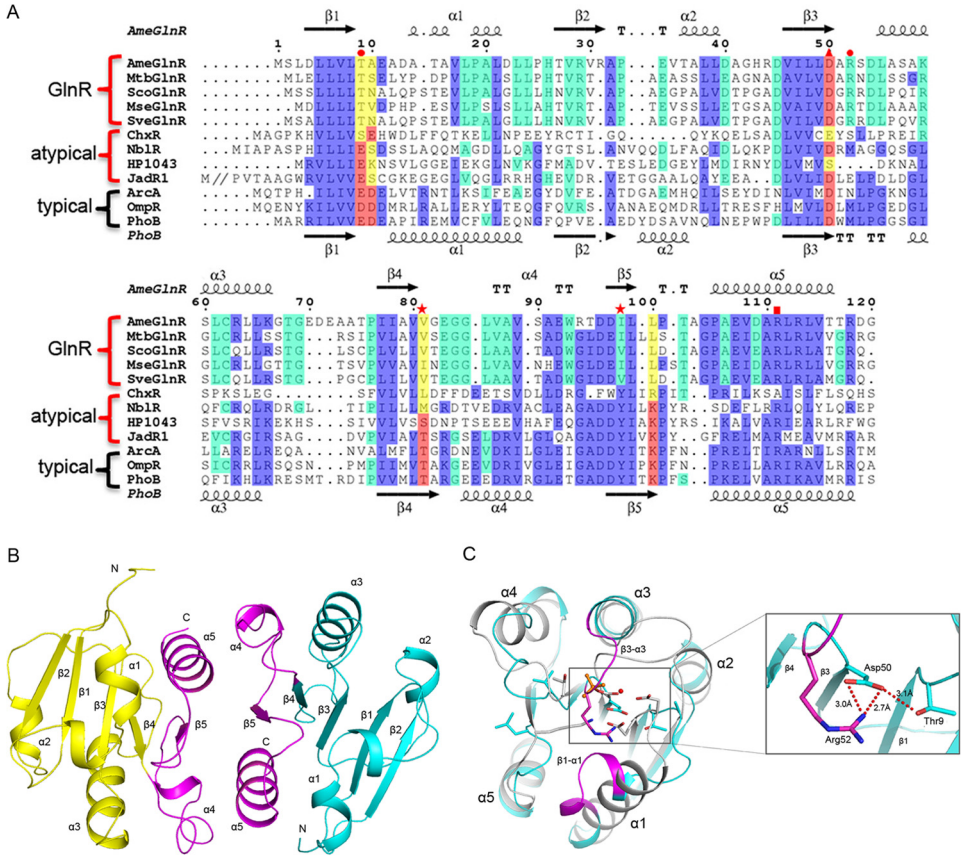

FIGURE 2. **Structure and comparison of different GlnRRecs.** *A*, structure-based sequence alignment of different GlnRRecs. The five residues constituting the phosphorylation pocket in typical RRs are highlighted in *red*, whereas the corresponding residues that differ from typical RRs in GlnR and atypical RRs are shown in *yellow*. The highly conserved residues among OmpR subfamily RRs are *colored* in *blue*, and the residues only showing conservation among GlnRs are *colored* in *cyan*. *Red stars*, conformation switch residues in typical RRs; *red triangle*, conserved residue Asp in the putative phosphorylation site; *red circles*, the two residues Thr and Arg forming interactions with the residue Asp in the putative phosphorylation site; *red square*, Arg residue essential for the dimerization. The secondary structure elements of AmeGlnRR and PhoB (Protein Data Bank code 1ZES) are shown at the *top* and *bottom*, respectively. *AmeGlnR*, GlnR from *A. mediterranei* U32 (YP_003771100); *MtbGlnR*, GlnR from *M. tuberculosis* H37Rv (NP_215333); *ScoGlnR*, GlnR from *S. coelicolor* M145 (NP_628336); *MseGlnR*, GlnR from *M. smegmatis strain* MC2 155 (YP_890012); *SveGlnR*, GlnR from *S. venezuelae* ATCC 10712 (YP006879462). ChxR is from *C. trachomatis* 434/Bu (YP_001654963); NblR is from *Synechococcus elongatus* PCC 7942(AAC33849); HP1043 is from *H. pylori* (NP_207833); JadR1 is from *S. venezuelae* ATCC 10712(AAB36584); ArcA is from *E. coli* K12 (NP_418818); OmpR is from *E. coli* O157:H7 strain EDL933 (NP_289945); and PhoB is from *E. coli* K12 (NP_414933). *B*, *ribbon diagram* shows the structure of the AmeGlnRRec. The two molecules A and B constituting the homodimer are *colored* in *yellow* and *cyan*, and the dimer interface is shown in *magenta*. *C*, structure comparison of AmeGlnRRec (*cyan*) with phosphorylated PhoB (*gray*) (Protein Data Bank code 1ZES). β1-α1 and β3-α3 loops and residue Arg^{52} of AmeGlnRRec are *colored* in *magenta*. The residues important for phosphorylation in PhoB and corresponding ones in AmeGlnRRec are shown with side chains. A *close-up view* of the putative phosphorylation pocket and interactions is also shown.

two residues, and the side chain of Asp^{50} may further be stabilized by forming another hydrogen bond with Thr^{9}. Thus, the configuration of Arg^{52} not only lessens the likelihood of residue Asp^{50} being phosphorylated but also introduces a hydrogen-bonding/ionic interaction network, which may provide an alternative mechanism for maintaining the homodimerization status of GlnR different from that of Asp phosphorylation in typical RRs (Fig. 2*C*).

Homodimerization of the Two GlnR Monomers through Their α4-β5-α5 Interface Is Essential for Their Physiological Function—The crystal structure data suggest that both AmeGlnRRec and MtbGlnRRec form homodimers. The interface involves the α4-β5-α5 secondary structure elements from both monomers and buries about 30% of the total surface area, which is similar to that of the phosphorylated typical RRs, such as PhoB and ArcA (Fig. 3, *A* and *B*), where homodimerization through such an interface is universal and essential for their physiological activities. On the other hand, in contrast to ArcA and PhoB, there is a lower percentage of hydrophilic residues but a higher percentage of hydrophobic residues within the interface of the two GlnR monomers, which presumably favors tighter protein-protein interactions (Fig. 3*A*). Two Arg^{111} residues in AmeGlnRRec from β5 of both monomers A and B, conserved among almost all OmpR/PhoB subfamily proteins except for the atypical ChxR from *Chlamydia trachomatis* (Fig. 2*A*), are found stacking against each other by π-π interactions. This Arg residue further stabilizes the interface by forming salt bridge and hydrogen bond networks with Asp^{97} and Glu^{107} from both monomers (Fig. 3*C*). The predominant role of this Arg residue in maintaining the homodimer is confirmed by site-directed mutagenesis analysis followed by gel filtration verification, in which an R111A single mutation results in a disruption of the homodimer of AmeGlnRRec (Fig. 3*D*). The hydrophilic interactions among Arg^{111}, Asp^{97}, and Glu^{107} are surrounded by hydrophobic residues Leu^{86}, Val^{89}, Ile^{98}, Ala^{106}, Ala^{110}, and Leu^{114}, which protrude from α4 and α5 helices of monomers A and B, strengthening the homodimer interaction (Fig. 3, *A* and *C*).

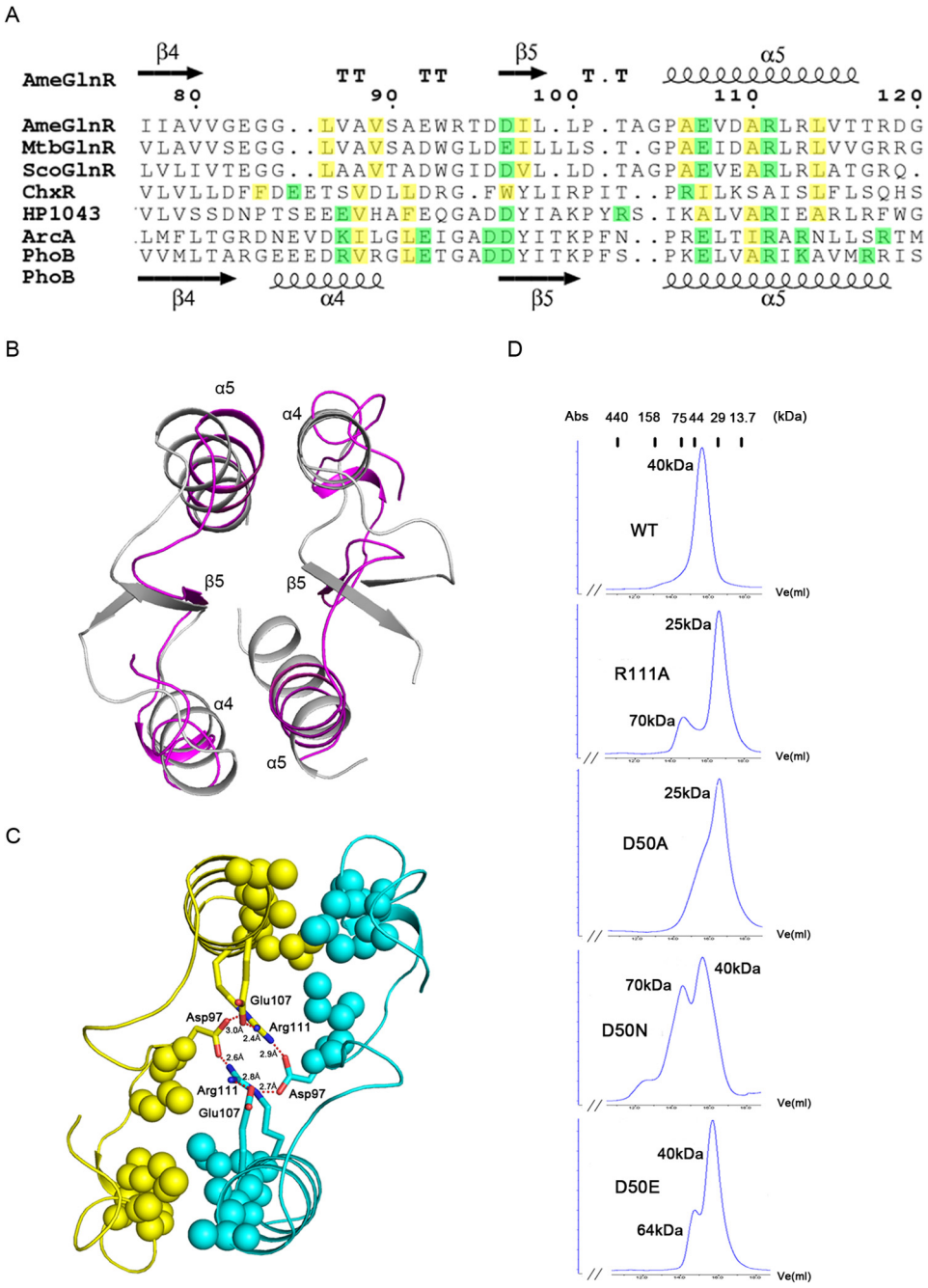

FIGURE 3. **Structure and *in vitro* characterization of the residues essential for AmeGlnRRec homodimer interaction.** *A*, sequence alignment of the residues constituting the dimer interface of GlnR, ChxR, HP1043, ArcA, PhoB, and the hydrophobic and hydrophilic residues are *colored* in *yellow* and *green*, respectively. *B*, superimposition of the structural elements involved in the homodimer interface of AmeGlnRRec (*magenta*) and PhoB (*gray*). *C*, residues involved in the homodimer formation. The two molecules are *colored* in *yellow* and *cyan*. Hydrophobic interaction residues are shown with *spheres*, and hydrophilic residues forming hydrogen bonds and salt bridges (shown with *red dashed lines* and *numbers* indicating the distance) are shown with side chains. *D*, gel filtration analysis of wild type AmeGlnRRec and its mutants. The mobility profiles of wild type AmeGlnRRec, R111A, D50A, D50N, and D50E are shown, and the molecular masses were calculated based on the standard proteins indicated at the *top*. The 25- and 40-kDa peaks represent the monomer and dimer, respectively, whereas the 64- and 70-kDa peaks represent the oligomer.

The dimerization and extensive interactions of the receiver domains imply that GlnR may form a homodimer as its functional status under physiological conditions. However, we failed in crystallization and analysis of the oligomeric state of the full-length GlnR using the heterogeneously expressed protein, probably due to its aggregation in solution. Alternatively, as shown in Fig. 4, we demonstrate that the AmeGlnR protein exists mainly as dimers *in vivo* in the presence of cross-linking agent DSS under either nitrogen-rich or limited conditions. We further explore whether the $\alpha4$-$\beta5$-$\alpha5$ interface is essential for the homodimerization of full-length AmeGlnR. Indeed, AmeGlnR harboring an R111A mutation changes the oligomeric state from dimers to monomers, which suggests that the homodimerization of AmeGlnR is dependent on the $\alpha4$-$\beta5$-$\alpha5$ interface *in vivo* (Fig. 4).

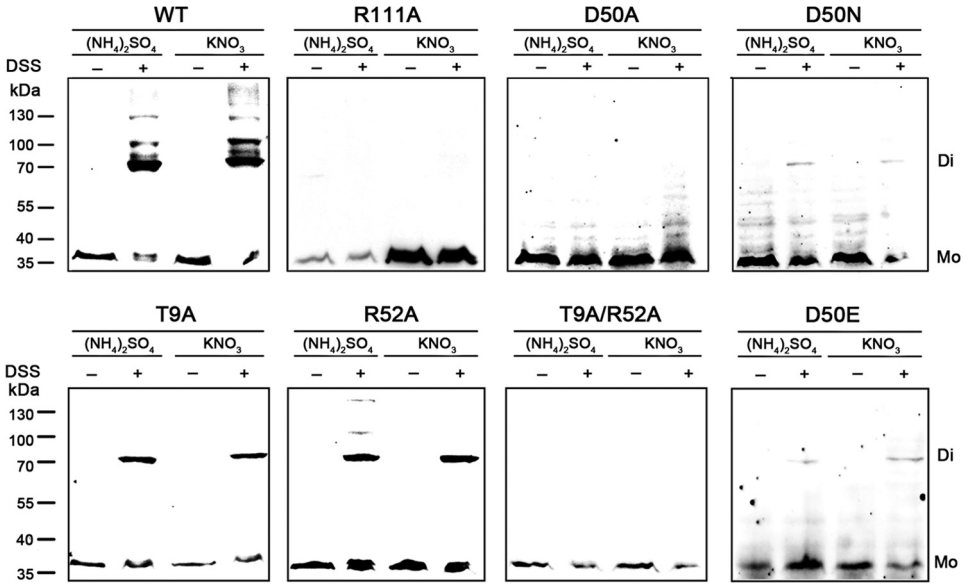

FIGURE 4. ***In vivo* cross-linking analysis of AmeGlnR and its mutants.** The oligomeric status of the wild type and mutated AmeGlnR (R111A, D50A, D50N, T9A, R52A, T9A/R52A, and D50E) in the presence (+) and absence (−) of cross-linking agent DSS are shown by Western blot analysis. The strains were cultured in the nitrogen-rich ($(NH_4)_2SO_4$) or -limited (KNO_3) conditions. Molecular markers are shown on the *left*. *Di*, dimer; *Mo*, monomer.

The *glnR* null mutants of both *A. mediterranei* U32 and *S. coelicolor* are proved unable to grow on minimal medium when nitrate is supplied as the sole nitrogen source (10, 39). Similar growth failure was observed when mutations of R111A/E (Fig. 5) or R108A/E (data not shown) were introduced individually into *AmeglnR* or *ScoglnR*, respectively. Consistent with these physiological phenotypes, the transcription of GlnR target genes, such as *nasA* and *glnA*, are not activated in *A. mediterranei glnR*(R111A/E) mutants either (Fig. 6). Further EMSA experiments using purified mutated proteins indicated that the DNA binding abilities of AmeGlnR(R111A) and AmeGlnR(R111E) proteins were all significantly reduced (Fig. 7). These data suggest that the homodimer formation through the $\alpha4$-$\beta5$-$\alpha5$ interface is indispensable for GlnR function *in vivo*, and the disruption of homodimer formation of GlnR may lead to the impairment of its DNA binding ability, therefore abolishing the regulatory function of GlnR.

The Conserved Asp^{50} of GlnR Is Critical for Maintaining the Receiver Domain-mediated Protein Dimerization and the Corresponding Physiological Function—The above biochemical and structural analyses clearly demonstrate that GlnR with the conserved Asp unphosphorylated is functional. However, because the D50A mutation supposed to mimic its unphosphorylated status of GlnR can neither complement for the growth defect of the *glnR* null mutants nor bind to its target promoter, such as that of *glnA* (Figs. 5 and 7; see Ref. 14 for the data of *M. smegmatis*), the underlying mechanism for the importance of Asp^{50} in maintaining the biological function of GlnR needs to be addressed.

The crystal structure of the wild type AmeGlnRRec protein indicates that Asp^{50} forms an ionic interaction with Arg^{52} and a hydrogen bond with Thr^{9} (Fig. 2*C*; see above). This is also true in the structure of MtbGlnRRec, in which Asp^{49} forms similar interactions with Arg^{51} and Thr^{8}. Therefore, we propose that these charge interactions may stabilize the homodimeric conformation of GlnR (Fig. 2*C*), and D50A mutation in AmeGlnR

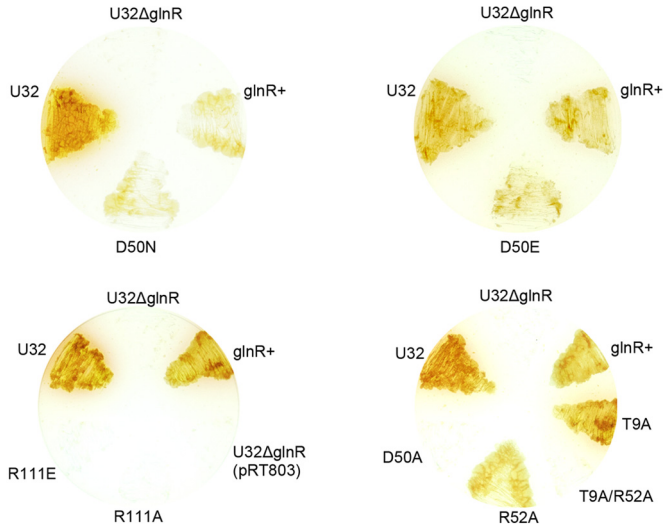

FIGURE 5. **Growth phenotypes of *A. mediterranei* U32 mutants and complementation strains.** Results of complementation by wild type *AmeglnR* or the *glnR* mutants (R111A/E, D50A, D50N, D50E, T9A, R52A, and T9A/R52A) grown on minimal medium supplemented with KNO_3.

may completely disrupt these interactions and thus result in dismantling the functional homodimerization.

The influence of this D50A mutation upon homodimer formation of either the AmeGlnRRec or the full-length AmeGlnR protein was verified using *in vitro* size exclusion chromatographic analysis or an *in vivo* chemical cross-linking assay, respectively. Both results suggest that whereas the wild type AmeGlnR forms homodimer, AmeGlnR(D50A) exists mainly as monomers (Figs. 3*D* and 4). To explore the possible mechanism underlying the effect of the D50A mutation upon dimerization, the structure of AmeGlnRRec(D50A) is modeled based on that of the wild type AmeGlnRRec through molecular dynamic (MD) simulations (Fig. 8). Comparing these two structural models, it is obvious that the Asp^{50}-focused charge interaction network (with Arg^{52} and Thr^{9}) is completely abolished

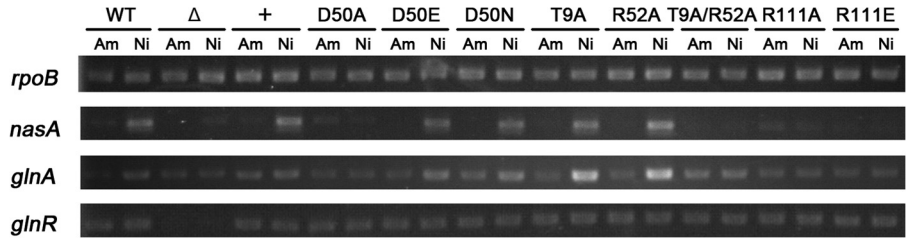

FIGURE 6. **Transcriptional analysis of wild type U32 and *glnR* mutants for the transcription of GlnR target genes in *A. mediterranei*.** The transcription of *rpoB* was used as the internal control. *WT*, wild type *A. mediterranei* U32; Δ, U32Δ*glnR*; +, *AmeglnR*+; *D50A*, *AmeglnR*(D50A); *D50E*, *AmeglnR*(D50E); *D50N*, *AmeglnR*(D50N); *T9A*, *AmeglnR*(T9A); *R52A*, *AmeglnR*(R52A); *T9A/R52A*, *AmeglnR*(T9A/R52A); *R111A*, *AmeglnR*(R111A); *R111E*, *AmeglnR*(R111E); *Am*, Bennett's medium with 60 mM ammonium; *Ni*, Bennett's medium with 80 mM KNO_3.

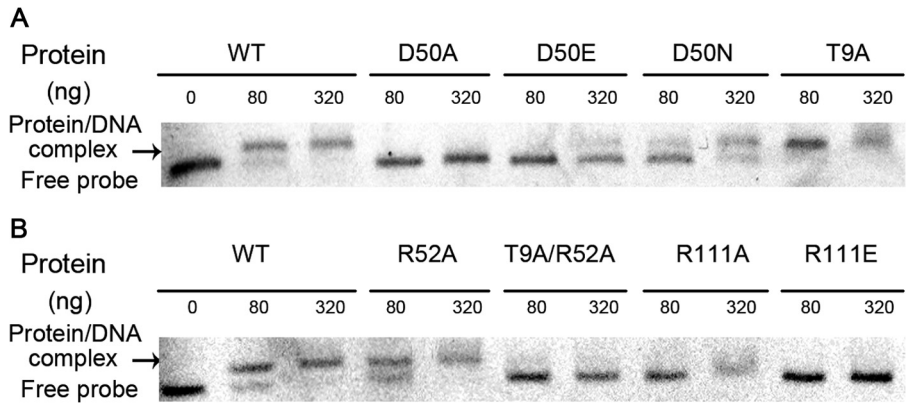

FIGURE 7. **EMSA results of wild type AmeGlnR and its mutants.** The FAM-labeled *glnA* promoter region was incubated with the indicated concentrations of AmeGlnR proteins (WT, D50A, D50E, D50N, T9A, R52A, T9A/R52A, R111A, and R111E), and salmon sperm DNA was added in each sample to mask the nonspecific binding effect. The signals of free DNA and protein-DNA complexes were scanned and shown.

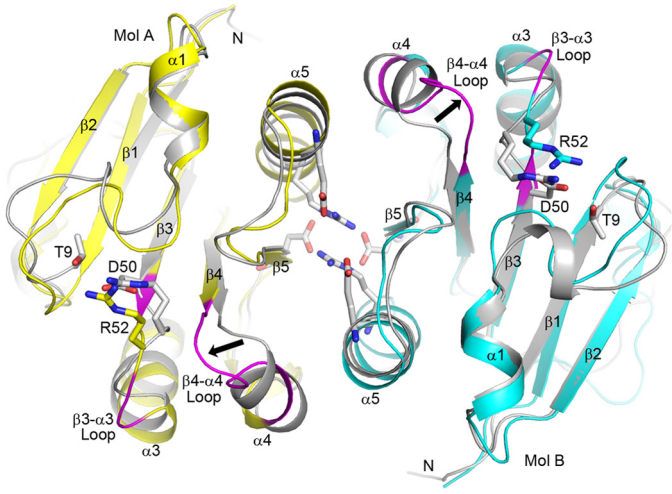

FIGURE 8. **Structural differences between wild type AmeGlnRRec dimer and AmeGlnRRec(D50A) (MD simulations).** The structure of wild type AmeGlnRRec dimer is *colored gray*, the MD simulated structure of AmeGlnRRec(D50A) is *colored yellow* (molecule A) and *cyan* (molecule B). The β3-α3 loop (residues Ala^{50}–Asp^{54}) and β4-α4 loop (residues Val^{81}–Val^{86}) are *colored* in *magenta*, and an *arrow* indicates the significant conformational change in β4-α4 loop. The residues constituting the putative phosphorylation pocket and the polar residues involved in the dimer interface are shown with *sticks*.

in the D50A mutant, which may cause both the Arg^{52} residue and the β3-α3 loop (residues Ala^{50}–Asp^{54}) to move away from the so-called "phosphorylation pocket," leaving a space to accommodate the β4-α4 loop (residues Val^{81}–Val^{86}) shifted away from the dimer interface (shown as arrows in Fig. 8). The conformational change in β4-α4 loop and the connecting α4 helix may greatly impair the α4-β5-α5 interface, through which the two monomers form a homodimer.

To further verify the above hypothesis, we generated two groups of mutants based on the structural information. The *AmeglnR*(D50N) and *AmeglnR*(D50E) mutants are designed to maintain the hydrogen bonds of either Asn^{50} or Glu^{50} with Arg^{52} and Thr^{9}, although the interactions are weakened due to the loss of the proposed salt bridge or the varied bond lengths in between. The AmeGlnR mutants containing either R52A or T9A alone and the double mutant of R52A/T9A belong to the second group, which is designed to test the effect of charge interactions by altering the surrounding amino acid residues individually or together rather than simply mutating the Asp^{50} residue as in the first group.

All of these mutants were tested for their *in vivo* oligomeric status, growth properties, and *in vitro* DNA binding capabilities. The AmeGlnR containing the single mutation of D50N, D50E, R52A, or T9A alone still forms a homodimer, whereas the GlnRs with either a single mutation of D50A or double mutation of T9A/R52A exist as monomers *in vivo* (Fig. 4). Consistently, the AmeGlnR proteins containing the D50N, D50E, R52A, or T9A mutation individually can bind to the *glnA* promoter *in vitro* and activate its transcription *in vivo*, whereas the D50A or T9A/R52A mutated AmeGlnR cannot (Figs. 6 and 7). Physiologically, as expected, the mutants of D50N, D50E, R52A, or T9A alone can complement the growth defect of the Δ*glnR* host on minimal medium supplemented with nitrate as the sole nitrogen source (Fig. 5), but neither AmeGlnR(D50A) nor AmeGlnR(R52A/T9A) mutant can. In addition, the AmeGlnR(D50L) mutant, which diminishes the charge interac-

tion completely as that of the D50A mutant but maintains the length of the side chain similar to that of Asp, is shown to completely impair the complementation function either (data not shown). It is also significant that similar results are obtained in *S. coelicolor* with corresponding mutations in ScoGlnR (data not shown). All of the above data suggest that the charge interactions among Asp^{50}, Arg^{52}, and Thr^{9} of AmeGlnR are critical for maintaining its receiver domain-mediated protein dimerization and the corresponding physiological function, which may be applied to the GlnRs of other actinomycetes.

DISCUSSION

The global transcription factor GlnR of the Gram-positive actinomycetes has been one of the major research focuses with respect to bacterial molecular physiology. It is due to not only its pivotal role in coordinating the expression of genes related to nitrogen metabolism of this industrially and medically important bacterial clade in response to the environmental nitrogen conditions but also its significantly different mode of action as an orphan RR in contrast to that of the well studied two-component system in Gram-negative enteric bacteria. However, the progress of the research has been largely hindered by the difficulties involved in biochemical determination and genetic characterization of GlnR phosphorylation status and its impact upon the protein's structure-function relationship under different physiological conditions. In this study, with a great deal of technological improvement, taking advantage of both the comprehensive research system developed in *A. mediterranei* and the highly conserved properties of GlnR from *S. coelicolor* and *M. tuberculosis*, multilevel evidence is gathered to support the conclusion that the actinomycete GlnR is an atypical OmpR/PhoB subfamily RR and functions as a homodimer stabilized by the critical charge interactions of the unphosphorylated conserved Asp residue with its spatially nearby polar amino acid residues.

Because of the universal presence of a so-called "phosphorylation pocket" within the N-terminal receiver domain of typical RRs, RRs without the pocket, usually determined by sequence alignment, are categorized as "atypical" and subject to various regulatory mechanisms different from that of phosphorylation at the conserved Asp residue in the "pocket" region (44). The crystal structures of AmeGlnRRec and MtbGlnRRec and the structure-based sequence alignment analysis presented in this study demonstrate that the actinomycete GlnR not only lacks the typical acidic pocket but also has the possibility of phosphorylation at the conserved Asp^{50} site being spatially excluded (Fig. 2). Therefore, in combination with the reproducible negative results in detecting the phosphorylated GlnR either *in vitro* or *in vivo* along with the clear positive controls, it is quite certain that the functional GlnR is not phosphorylated at its conserved aspartate residue (Fig. 1). However, this residue is still essential for the physiological function of AmeGlnR, as shown both *in vitro* and i*n vivo* in this study (Fig. 5).

Usually the Glu/Ala mutation at the conserved phospho-accepting Asp residue is known to mimic the phosphorylation/unphosphorylation status of the RRs (45, 46), although exceptions do exist. For instance, the Asp → Glu mutant of VirG, an RR of the VirA/VirG two-component system in *Agrobacterium tumefaciens*, does not mimic the phenotype of the phosphorylated VirG. In fact, this study offers another case, where, in contrast to the completely deficient GlnR(D50A) mutant, the GlnR(D50N) is still functional, which is another frequently used mimetic model for the unphosphorylated status. Therefore, these mutations are useful models for mechanistic studies rather than for the proof of the presence of phosphorylation.

The current understanding of the mechanism of activation of the typical RRs is derived from comparisons of structures under the phosphorylated *versus* the unphosphorylated states (3, 8). For most of the typical RRs, the phosphorylation at their Asp residues induces conformational changes. Particularly, the reorientation of the $\beta4$-$\alpha4$ loop and the two conserved switch residues, namely Ser/Thr from $\beta4$ and Tyr/Phe from $\beta5$, are changed to facilitate the transition of the RR from monomers (47–49) or weak dimers (2), both at their unphosphorylated states, to the "tight" functional homodimers through the formation of a common $\alpha4$-$\beta5$-$\alpha5$ ionic interface contributed by a set of highly conserved residues. This strong interaction further brings the DNA binding domains into close proximity, allowing them to bind to the direct repeat half-sites that comprise the recognition sequences for most OmpR/PhoB subfamily RRs (3, 50). On the other hand, the crystal structure of the orphan RR GlnR, unphosphorylated at the conserved Asp residue, forms a functional homodimer through the $\alpha4$-$\beta5$-$\alpha5$ interface, which is in accordance with the previous data regarding the GlnR binding consensus sequences, where two GlnR binding boxes are found in many cases (18, 51).

Various mechanisms are adopted for facilitating and stabilizing the functional dimerization in atypical RRs in addition to the universal $\alpha4$-$\beta5$-$\alpha5$ secondary structure element critical for a proper interface. First of all, both ionic and hydrophobic interactions within the dimer interface are employed as the main forces for stabilizing the functional dimer. In the cases of HP1043 from *Helicobacter pylori* and ChxR from *C. trachomatis*, no matter whether the conserved Arg residue (corresponding to Arg^{111} of AmeGlnR) is present in the former or absent in the latter, they all retain the conserved Tyr residues as in typical RRs as well as a few atypical RRs (Fig. 2*A*), and the side chains in both cases adopted a similar orientation toward the active site as that of the phosphorylated typical RRs in order to facilitate the formation of active dimers. In contrast, the $\alpha4$ helix of AmeGlnRRec is partially unwound, and the residues corresponding to Ser/Thr and Tyr/Phe in typical RRs are replaced by Val^{81} and Ile^{98}, the side chains of which adopt similar orientations as that of the unphosphorylated typical RRs (Fig. 9). However, the smaller side chain of Ile^{98}, compared with that of Tyr/Phe, may allow a close interaction between the two monomers through the $\alpha4$-$\beta5$-$\alpha5$ interface, which is highly similar to that of the phosphorylated typical RRs. In fact, similar small side chain residues are found in the GlnR proteins from various actinomycetes (Fig. 2*A*), which suggests that a dimer-stabilizing mechanism distinct from that of HP1043 and ChxR is commonly adopted.

More significantly, along with resolving the controversial mutational analysis upon the conserved Asp residue within the missing "phosphorylation pocket" quintet of actinomycete GlnR, this study demonstrates that this Asp residue plays an

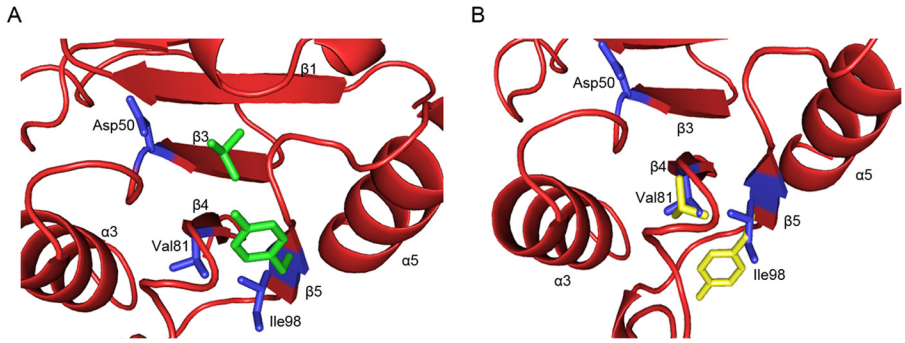

FIGURE 9. **Different conformations of the "switch residues" in AmeGlnRRec and PhoB.** The conformations of the "switch residues" in AmeGlnRRec (Val^{81} and Ile^{98}, shown with *blue sticks*) differ from those in phosphorylated PhoB (*green sticks*) (*A*) but are similar to those in unphosphorylated PhoB (*yellow stick*) (*B*). The Protein Data Bank codes of phosphorylated and unphosphorylated PhoB are 1ZES and 1B00, respectively.

important role in maintaining the functional conformation of the active homodimer via the formation of salt bridge/hydrogen bond interactions with two spatially close Arg and Thr residues (Thr^{9}-Asp^{50}-Arg^{52} interactions). This unique mechanism, novel among all of the atypical RRs studied so far, is comprehensively verified by mutational analysis, detecting their dimerization capabilities as well as related functional impacts both *in vitro* and *in vivo*. In addition, the MD simulation for wild type and all of the mutants indicates that a significant conformational difference that occurs in the $\beta4$-$\alpha4$ loop is only observed in the GlnR(D50A) (Fig. 8) and GlnR(D50L) (data not shown) mutants, where the loop shifts toward the Asp^{50} position and may consequently influence or even disable the homodimerization of GlnR via weakening the $\alpha4$-$\beta5$-$\alpha5$ dimer interface. Interestingly, upon phosphorylation/dephosphorylation, the $\beta4$-$\alpha4$ loop of the typical PhoB actually undergoes significant rearrangement, changing PhoB from homodimers to monomers, respectively. The spatial position of the loop in the unphosphorylated PhoB is the same as that in GlnR(D50A) (3), which may therefore explain the negative effect of D50A mutation upon the oligomerization of GlnR.

So far, this study has shown that the actinomycete GlnR is not phosphorylated at the conserved Asp residue *in vitro* or *in vivo* and thus is confirmed to be an atypical RR. Further RT-PCR analyses employing two GlnR target genes, *nasA* and *glnA*, show that the transcriptional activation ability of the AmeGlnR mutants is consistent with their corresponding growth phenotypes (Fig. 6); *i.e.* the active GlnR mutants, GlnR(D50E), GlnR(D50N), GlnR(T9A), and GlnR(R52A) are still able to respond to the extracellular nitrogen availabilities, whereas the inactive GlnR mutants, GlnR(D50A), GlnR(T9A/R52A), and GlnR(R111A/E), are not.

It is known that apart from the possible post-translational modification, transcription of the *S. coelicolor glnR* gene is stringently regulated by the environmental nitrogen availability (10), which may alter the quantity of functional GlnR available *in vivo*. However, the expression of *glnR* in *A. mediterranei* and *M. smegmatis* is not significantly affected by the extracellular nitrogen sources (15, 25). Considering the fact that the biological function of the above GlnRs is only found in nitrogen-limited conditions, at least the GlnRs of *A. mediterranei* and *M. smegmatis* are expected to be regulated by uncharacterized mechanisms, most likely post-translational modification, resulting in distinct activities in GlnR-mediated global transcriptional regulation. Although eukaryotic phosphorylation on Ser, Thr, or Tyr residues, often identified in prokaryotic proteins (52), is seemingly excluded by the Phos-tag assays under our tested conditions, in addition to that of the Asp residue, it might occur under other cultural conditions or detected by other assay methods. Meanwhile, other types of modifications besides phosphorylation have been reported to alter the activities of atypical RRs (*e.g.* posttranslational acetylation of RcsB (53, 54) and binding of the small ligand jadomycin B in the modulation of the JadR1 from *Streptomyces venezuelae* (44)). Interestingly, in the two cases mentioned above, although different mechanisms are adopted, they both inactivate rather than activate the atypical transcription factors under certain metabolic conditions. In the case of actinomycete GlnR, which is naturally active in its dimer status that is stabilized by a robust charge interaction network, "activation" of GlnR seems unnecessary, whereas a similar "inactivation" consequence conveyed by its special regulation mechanism(s) is expected under nitrogen-rich conditions. Therefore, efforts are currently under way in that direction.

Acknowledgment—We thank the staff at the Shanghai synchrotron facility beamline 17U1 for technical assistance with data collection.

REFERENCES

1. Stock, A. M., Robinson, V. L., and Goudreau, P. N. (2000) Two-component signal transduction. *Annu. Rev. Biochem.* **69,** 183–215
2. Gao, R., and Stock, A. M. (2009) Biological insights from structures of two-component proteins. *Annu. Rev. Microbiol.* **63,** 133–154
3. Bachhawat, P., Swapna, G. V., Montelione, G. T., and Stock, A. M. (2005) Mechanism of activation for transcription factor PhoB suggested by different modes of dimerization in the inactive and active states. *Structure* **13,** 1353–1363
4. Jeon, Y., Lee, Y. S., Han, J. S., Kim, J. B., and Hwang, D. S. (2001) Multimerization of phosphorylated and non-phosphorylated ArcA is necessary for the response regulator function of the Arc two-component signal transduction system. *J. Biol. Chem.* **276,** 40873–40879
5. Chen, Y., Birck, C., Samama, J. P., and Hulett, F. M. (2003) Residue R113 is essential for PhoP dimerization and function: a residue buried in the asymmetric PhoP dimer interface determined in the PhoPN three-dimensional crystal structure. *J. Bacteriol.* **185,** 262–273
6. Mack, T. R., Gao, R., and Stock, A. M. (2009) Probing the roles of the two different dimers mediated by the receiver domain of the response regulator PhoB. *J. Mol. Biol.* **389,** 349–364

7. Hong, E., Lee, H. M., Ko, H., Kim, D. U., Jeon, B. Y., Jung, J., Shin, J., Lee, S. A., Kim, Y., Jeon, Y. H., Cheong, C., Cho, H. S., and Lee, W. (2007) Structure of an atypical orphan response regulator protein supports a new phosphorylation-independent regulatory mechanism. *J. Biol. Chem.* **282,** 20667–20675
8. Kern, D., Volkman, B. F., Luginbühl, P., Nohaile, M. J., Kustu, S., and Wemmer, D. E. (1999) Structure of a transiently phosphorylated switch in bacterial signal transduction. *Nature* **402,** 894–898
9. Amon, J., Titgemeyer, F., and Burkovski, A. (2010) Common patterns, unique features: nitrogen metabolism and regulation in Gram-positive bacteria. *FEMS Microbiol. Rev.* **34,** 588–605
10. Tiffert, Y., Supra, P., Wurm, R., Wohlleben, W., Wagner, R., and Reuther, J. (2008) The *Streptomyces coelicolor* GlnR regulon: identification of new GlnR targets and evidence for a central role of GlnR in nitrogen metabolism in actinomycetes. *Mol. Microbiol.* **67,** 861–880
11. Malm, S., Tiffert, Y., Micklinghoff, J., Schultze, S., Joost, I., Weber, I., Horst, S., Ackermann, B., Schmidt, M., Wohlleben, W., Ehlers, S., Geffers, R., Reuther, J., and Bange, F. C. (2009) The roles of the nitrate reductase NarGHJI, the nitrite reductase NirBD and the response regulator GlnR in nitrate assimilation of *Mycobacterium tuberculosis*. *Microbiology* **155,** 1332–1339
12. Tullius, M. V., Harth, G., and Horwitz, M. A. (2003) Glutamine synthetase GlnA1 is essential for growth of *Mycobacterium tuberculosis* in human THP-1 macrophages and guinea pigs. *Infect. Immun.* **71,** 3927–3936
13. Zhao, W., Zhong, Y., Yuan, H., Wang, J., Zheng, H., Wang, Y., Cen, X., Xu, F., Bai, J., Han, X., Lu, G., Zhu, Y., Shao, Z., Yan, H., Li, C., Peng, N., Zhang, Z., Zhang, Y., Lin, W., Fan, Y., Qin, Z., Hu, Y., Zhu, B., Wang, S., Ding, X., and Zhao, G. P. (2010) Complete genome sequence of the rifamycin SV-producing *Amycolatopsis mediterranei* U32 revealed its genetic characteristics in phylogeny and metabolism. *Cell Res.* **20,** 1096–1108
14. Jenkins, V. A., Robertson, B. D., and Williams, K. J. (2012) Aspartate D48 is essential for the GlnR-mediated transcriptional response to nitrogen limitation in *Mycobacterium smegmatis*. *FEMS Microbiol. Lett.* **330,** 38–45
15. Yu, H., Yao, Y., Liu, Y., Jiao, R., Jiang, W., and Zhao, G. P. (2007) A complex role of *Amycolatopsis mediterranei* GlnR in nitrogen metabolism and related antibiotics production. *Arch. Microbiol.* **188,** 89–96
16. Tiffert, Y., Franz-Wachtel, M., Fladerer, C., Nordheim, A., Reuther, J., Wohlleben, W., and Mast, Y. (2011) Proteomic analysis of the GlnR-mediated response to nitrogen limitation in *Streptomyces coelicolor* M145. *Appl. Microbiol. Biotechnol.* **89,** 1149–1159
17. Wang, Y., Cen, X. F., Zhao, G. P., and Wang, J. (2012) Characterization of a new GlnR binding box in the promoter of amtB in *Streptomyces coelicolor* inferred a PhoP/GlnR competitive binding mechanism for transcriptional regulation of amtB. *J. Bacteriol.* **194,** 5237–5244
18. Wang, J., and Zhao, G. P. (2009) GlnR positively regulates nasA transcription in *Streptomyces coelicolor*. *Biochem. Biophys. Res. Commun.* **386,** 77–81
19. Wang, Y., Wang, J. Z., Shao, Z. H., Yuan, H., Lu, Y. H., Jiang, W. H., Zhao, G. P., and Wang, J. (2013) Three of four GlnR binding sites are essential for GlnR-mediated activation of transcription of the *Amycolatopsis mediterranei* nas operon. *J. Bacteriol.* **195,** 2595–2602
20. Fink, D., Weissschuh, N., Reuther, J., Wohlleben, W., and Engels, A. (2002) Two transcriptional regulators GlnR and GlnRII are involved in regulation of nitrogen metabolism in *Streptomyces coelicolor* A3(2). *Mol. Microbiol.* **46,** 331–347
21. Hutchings, M. I., Hoskisson, P. A., Chandra, G., and Buttner, M. J. (2004) Sensing and responding to diverse extracellular signals? Analysis of the sensor kinases and response regulators of *Streptomyces coelicolor* A3(2). *Microbiology* **150,** 2795–2806
22. Bourret, R. B. (2010) Receiver domain structure and function in response regulator proteins. *Curr. Opin. Microbiol.* **13,** 142–149
23. Hickey, J. M., Lovell, S., Battaile, K. P., Hu, L., Middaugh, C. R., and Hefty, P. S. (2011) The atypical response regulator protein ChxR has structural characteristics and dimer interface interactions that are unique within the OmpR/PhoB subfamily. *J. Biol. Chem.* **286,** 32606–32616
24. O'Connor, T. J., and Nodwell, J. R. (2005) Pivotal roles for the receiver domain in the mechanism of action of the response regulator RamR of *Streptomyces coelicolor*. *J. Mol. Biol.* **351,** 1030–1047
25. Amon, J., Bräu, T., Grimrath, A., Hänssler, E., Hasselt, K., Höller, M., Jessberger, N., Ott, L., Szököl, J., Titgemeyer, F., and Burkovski, A. (2008) Nitrogen control in *Mycobacterium smegmatis*: nitrogen-dependent expression of ammonium transport and assimilation proteins depends on the OmpR-type regulator GlnR. *J. Bacteriol.* **190,** 7108–7116
26. Bertani, G. (2004) Lysogeny at mid-twentieth century: P1, P2, and other experimental systems. *J. Bacteriol.* **186,** 595–600
27. Mejía, A., Barrios-González, J., and Viniegra-González, G. (1998) Overproduction of rifamycin B by *Amycolatopsis mediterranei* and its relationship with the toxic effect of barbital on growth. *J. Antibiot.* **51,** 58–63
28. Kieser, T., and Hopwood, D. A. (1991) Genetic manipulation of *Streptomyces*: integrating vectors and gene replacement. *Methods Enzymol.* **204,** 430–458
29. Ma, J., Zhang, P., Zhang, Z., Zha, M., Xu, H., Zhao, G., and Ding, J. (2008) Molecular basis of the substrate specificity and the catalytic mechanism of citramalate synthase from *Leptospira interrogans*. *Biochem. J.* **415,** 45–56
30. Boulanger, A., Chen, Q., Hinton, D. M., and Stibitz, S. (2013) *In vivo* phosphorylation dynamics of the *Bordetella pertussis* virulence-controlling response regulator BvgA. *Mol. Microbiol.* **88,** 156–172
31. Sheridan, R. C., McCullough, J. F., Wakefield, Z. T. (1971) Phosphoramidic acid and its salts. *Inorg. Synth.* **13,** 23–26
32. Kinoshita, E., Kinoshita-Kikuta, E., Takiyama, K., and Koike, T. (2006) Phosphate-binding tag, a new tool to visualize phosphorylated proteins. *Mol. Cell Proteomics* **5,** 749–757
33. Barbieri, C. M., and Stock, A. M. (2008) Universally applicable methods for monitoring response regulator aspartate phosphorylation both *in vitro* and *in vivo* using Phos-tag-based reagents. *Anal. Biochem.* **376,** 73–82
34. Adams, P. D., Grosse-Kunstleve, R. W., Hung, L. W., Ioerger, T. R., McCoy, A. J., Moriarty, N. W., Read, R. J., Sacchettini, J. C., Sauter, N. K., and Terwilliger, T. C. (2002) PHENIX: building new software for automated crystallographic structure determination. *Acta Crystallogr. D Biol. Crystallogr.* **58,** 1948–1954
35. Emsley, P., and Cowtan, K. (2004) Coot: model-building tools for molecular graphics. *Acta Crystallogr. D Biol. Crystallogr.* **60,** 2126–2132
36. Hess, B., Kutzner, C., van der Spoel, D., and Lindahl, E. (2008) GROMACS 4: algorithms for highly efficient, load-balanced, and scalable molecular simulation. *J. Chem. Theory. Comput.* **4,** 435–447
37. Piana, S., Lindorff-Larsen, K., and Shaw, D. E. (2011) How robust are protein folding simulations with respect to force field parameterization. *Biophys. J.* **100,** L47–L49
38. Bussi, G., Donadio, D., and Parrinello, M. (2007) Canonical sampling through velocity rescaling. *J. Chem. Phys.* **126,** 014101
39. Yu, H., Peng, W. T., Liu, Y., Wu, T., Yao, Y. F., Cui, M. X., Jiang, W. H., and Zhao, G. P. (2006) Identification and characterization of glnA promoter and its corresponding trans-regulatory protein GlnR in the rifamycin SV producing actinomycete, *Amycolatopsis mediterranei* U32. *Acta Biochim. Biophys. Sin.* **38,** 831–843
40. Ding, X. M., Zhang, N., Tian, Y. Q., Jiang, W. H., Zhao, G. P., and Jiao, R. S. (2002) Establishment of gene replacement/disruption system through homologous recombination in *Amycolatopsis mediterranei* U32. *Sheng Wu Gong Cheng Xue Bao* **18,** 431–437
41. Shu, D., Chen, L., Wang, W., Yu, Z., Ren, C., Zhang, W., Yang, S., Lu, Y., and Jiang, W. (2009) afsQ1-Q2-sigQ is a pleiotropic but conditionally required signal transduction system for both secondary metabolism and morphological development in *Streptomyces coelicolor*. *Appl. Microbiol. Biotechnol.* **81,** 1149–1160
42. McCleary, W. R. (1996) The activation of PhoB by acetylphosphate. *Mol. Microbiol.* **20,** 1155–1163
43. Darbon, E., Martel, C., Nowacka, A., Pegot, S., Moreau, P. L., and Virolle, M. J. (2012) Transcriptional and preliminary functional analysis of the six genes located in divergence of phoR/phoP in *Streptomyces lividans*. *Appl. Microbiol. Biotechnol.* **95,** 1553–1566
44. Wang, L., Tian, X., Wang, J., Yang, H., Fan, K., Xu, G., Yang, K., and Tan, H. (2009) Autoregulation of antibiotic biosynthesis by binding of the end product to an atypical response regulator. *Proc. Natl. Acad. Sci. U.S.A.* **106,** 8617–8622
45. Gao, R., Mukhopadhyay, A., Fang, F., and Lynn, D. G. (2006) Constitutive activation of two-component response regulators: characterization of

VirG activation in *Agrobacterium tumefaciens*. *J. Bacteriol.* **188,** 5204–5211
46. Arribas-Bosacoma, R., Kim, S. K., Ferrer-Orta, C., Blanco, A. G., Pereira, P. J., Gomis-Rüth, F. X., Wanner, B. L., Coll, M., and Solà, M. (2007) The X-ray crystal structures of two constitutively active mutants of the *Escherichia coli* PhoB receiver domain give insights into activation. *J. Mol. Biol.* **366,** 626–641
47. Friedland, N., Mack, T. R., Yu, M., Hung, L. W., Terwilliger, T. C., Waldo, G. S., and Stock, A. M. (2007) Domain orientation in the inactive response regulator *Mycobacterium tuberculosis* MtrA provides a barrier to activation. *Biochemistry* **46,** 6733–6743
48. Nowak, E., Panjikar, S., Konarev, P., Svergun, D. I., and Tucker, P. A. (2006) The structural basis of signal transduction for the response regulator PrrA from *Mycobacterium tuberculosis*. *J. Biol. Chem.* **281,** 9659–9666
49. Robinson, V. L., Wu, T., and Stock, A. M. (2003) Structural analysis of the domain interface in DrrB, a response regulator of the OmpR/PhoB subfamily. *J. Bacteriol.* **185,** 4186–4194
50. West, A. H., and Stock, A. M. (2001) Histidine kinases and response regulator proteins in two-component signaling systems. *Trends. Biochem. Sci.* **26,** 369–376
51. Lewis, R. A., Shahi, S. K., Laing, E., Bucca, G., Efthimiou, G., Bushell, M., and Smith, C. P. (2011) Genome-wide transcriptomic analysis of the response to nitrogen limitation in *Streptomyces coelicolor* A3(2). *BMC Res. Notes* **4,** 78
52. Appleby, J. L., and Bourret, R. B. (1999) Activation of CheY mutant D57N by phosphorylation at an alternative site, Ser-56. *Mol. Microbiol.* **34,** 915–925
53. Thao, S., Chen, C. S., Zhu, H., and Escalante-Semerena, J. C. (2010) Nepsilon-lysine acetylation of a bacterial transcription factor inhibits Its DNA-binding activity. *PLoS. One* **5,** e15123
54. Hu, L. I., Chi, B. K., Kuhn, M. L., Filippova, E. V., Walker-Peddakotla, A. J., Bäsell, K., Becher, D., Anderson, W. F., Antelmann, H., and Wolfe, A. J. (2013) Acetylation of the response regulator RcsB controls transcription from a small RNA promoter. *J. Bacteriol.* **195,** 4174–4186